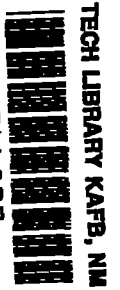


10518 81501
NACA TN 4179

0066897



NATIONAL ADVISORY COMMITTEE FOR AERONAUTICS

TECHNICAL NOTE 4179

ANALYTICAL INVESTIGATION OF ACCELERATION RESTRICTION IN
A FIGHTER AIRPLANE WITH AN AUTOMATIC CONTROL SYSTEM

By James T. Matthews, Jr.

Langley Aeronautical Laboratory
Langley Field, Va.



Washington
January 1958

AFMDC
TECHNICAL LIBRARY
JAN 2011



0066897

NATIONAL ADVISORY COMMITTEE FOR AERONAUTICS

TECHNICAL NOTE 4179

ANALYTICAL INVESTIGATION OF ACCELERATION RESTRICTION IN
A FIGHTER AIRPLANE WITH AN AUTOMATIC CONTROL SYSTEM

By James T. Matthews, Jr.

SUMMARY

A theoretical analysis was made to investigate the performance and acceleration-restriction capabilities of a normal-acceleration command control system in a fighter airplane. Several combinations of pitching velocity and pitching acceleration were investigated as feedback quantities in combination with normal acceleration.

The flight conditions considered were airspeeds of 600 and 1,000 feet per second, at sea level and an altitude of 20,000 feet, and maneuver margins of 3.3, 13.3, and 23.3 percent of the mean aerodynamic chord. The most desirable transient responses (10 percent or less overshoot) to acceleration commands were obtained when pitching velocity was fed back in a manner that increased the damping of the airplane and pitching acceleration was fed back in a manner that increased the effective inertia of the airplane. In order to obtain satisfactory performance, all the systems investigated required a compensating network which reduced the phase lag of the power control in the vicinity of its natural frequency.

The analysis also included the normal-acceleration response of the controlled airplane to simulated rough air. The normal-acceleration response of the controlled airplane to rough air was somewhat reduced as compared with that of the basic airplane, particularly at the lower maneuver margins. The magnitude of the pitching-velocity response was greater for the controlled airplane, as might be expected.

INTRODUCTION

In several previous reports (refs. 1, 2, and 3) acceleration restrictors have been analyzed which utilize the principle of stopping the elevator motion in accordance with a signal that depends upon longitudinal response quantities such as normal acceleration, pitching velocity, and pitching acceleration. The possibility has also been pointed out of obtaining acceleration restriction by limiting the input of an automatic

control system which is designed to produce a normal-acceleration response equal to the command. A normal-acceleration control system was analyzed in reference 4 and was shown to have desirable characteristics from the standpoint of rapid response to the pilot's control.

In the present report, consideration is given to certain features intended to improve the acceleration-limiting characteristics of a normal-acceleration control system. The characteristics desired are a rapid approach to the command value of normal acceleration with no overshoot and a steady-state response which closely approaches the command value. In order to attain these characteristics, pitching-acceleration feedback to reduce the effective inertia of the airplane in pitch and pitching-velocity feedback to increase the damping were investigated in combination with normal-acceleration feedback. The gust responses of these systems were also investigated. The results presented were obtained primarily with the aid of analog-computing equipment.

SYMBOLS

a_n	normal acceleration, g units
$a_{n,i}$	normal-acceleration input, g units
$\dot{a}_{n,i}$	rate of normal-acceleration input, $\frac{\text{g units}}{\text{sec}}$
$a_{n,o}$	normal-acceleration output, g units
\bar{c}	mean aerodynamic chord, ft
g	acceleration due to gravity, ft/sec ²
$j = \sqrt{-1}$	
K_1	forward-loop gain (ratio of elevator deflection to normal-acceleration error), $\frac{\text{radians}}{\text{g unit}}$
K_2	inner-loop gain (ratio of elevator deflection to pitching acceleration), $\frac{\text{radians}}{\text{radians/sec}^2}$
K_3	inner-loop gain (ratio of elevator deflection to pitching velocity), $\frac{\text{radians}}{\text{radians/sec}}$

V	airspeed, ft/sec
α_g	angle-of-attack change due to gusts, radians
δ_e	elevator deflection, radians
$\dot{\theta}$	pitching velocity, radians/sec
$\ddot{\theta}$	pitching acceleration, radians/sec ²
ω	circular frequency, radians/sec

ANALYSIS

Ideally, an acceleration restrictor should allow the airplane complete maneuvering freedom up to the point that has been chosen as the acceleration limit. Perfect limiting of acceleration at all flight conditions would be nearly impossible for a high-performance airplane; therefore a compromise must be reached. In this study the following conditions were assumed as the requirements:

(1) A maximum rate of normal-acceleration input of 6g per second (A brief check of many actual time histories of normal acceleration measured in flight during pull-ups indicated that 6g per second was a reasonable maximum rate.)

(2) A maximum allowable overshoot of about 10 percent of desired value

(3) Well damped transients (0.6 critical damping or greater) in normal acceleration

(4) Moderately damped transients in higher frequency modes which are predominant in pitching velocity and elevator motion (0.3 critical damping or greater)

In this section and in subsequent sections of this paper, the various normal-acceleration control systems considered are for convenience designated by certain symbols. The symbols $\dot{\theta}$ and $\ddot{\theta}$, when used in conjunction with the symbol a_n , indicate the inner-loop feedback quantity. The sign indicates whether the feedback is positive or negative. For example, " $a_n + \dot{\theta}$ control" indicates a normal-acceleration control system with positive pitching-acceleration feedback in the inner loop. The use of $\ddot{\theta}$ feedback changes the effective damping of the airplane

whereas $\ddot{\theta}$ feedback changes the effective inertia of the air flow. In either case positive feedback would be expected to decrease and negative feedback to increase the stability of the airplane-control-system combination. The characteristics of the subsonic jet fighter airplane used in this analysis are given in reference 1.

Block diagrams of the $a_n - \dot{\theta}$ and $a_n + \ddot{\theta}$ control systems are shown in figure 1. In the analysis of the a_n , $a_n - \dot{\theta}$, and $a_n + \ddot{\theta}$ control systems, ideal power control characteristics (no lag) were assumed. The forward-loop gain K_1 was varied through a reasonable range. The pitching-velocity feedback gain was selected so as to double the damping of the basic airplane, whereas the pitching-acceleration feedback gains were selected so that for each value of the forward-loop gain the effective inertia of the airplane was reduced to zero. The effectiveness of the systems studied as acceleration restrictors was determined from transient responses to ramp inputs. Results were obtained over a range of values of airspeed and with values of maneuver margin of 3.3, 13.3, and 23.3 percent of the mean aerodynamic chord.

Power-control dynamics, stabilizing and integrating networks, and various positive and negative combinations of the feedback quantities $\dot{\theta}$ and $\ddot{\theta}$ were investigated. A composite block diagram of these systems is shown in figure 2. For the purposes of this analysis the power control was assumed to have a natural frequency of 30 radians per second and a damping ratio of 0.5 of critical damping.

The effectiveness of the various normal-acceleration control systems as acceleration restrictors was determined from transient responses to ramp-type acceleration commands. An analog computer was utilized to simulate the dynamics of the various components in order to obtain the transient responses to an acceleration command input which increased linearly from 0 to 1 g at the rate of 6g per second. The transient responses were obtained for several flight conditions at sea level. These conditions were airspeeds of 600 and 1,000 feet per second and three center-of-gravity locations corresponding to maneuver margins of 3.3, 13.3, and 23.3 percent of the mean aerodynamic chord. In order to investigate an airplane with reduced damping, flying at a higher altitude, the same conditions were assumed except that all the damping derivatives were reduced by a factor of 2 and the altitude was 20,000 feet. Some of the effects of gusts on an airplane equipped with a normal-acceleration control system were also studied. Frequency responses due to sinusoidal gusts for the ideal systems of figure 1 were calculated. Unsteady lift effects were neglected in the calculations. In the analysis simulated rough air was introduced into the analog computer by a motor-driven cam containing 24 discrete frequencies of constant amplitude. The cam output was then integrated in the process of going through the computer, and the result was a rough-air input whose amplitude varied inversely with frequency. This input

approximates the amplitude variation with frequency corresponding to the continuous power spectrum of atmospheric turbulence, as indicated by the results of reference 5.

RESULTS AND DISCUSSION

Acceleration-Restriction Results

The results of the preliminary calculations, which assumed ideal power control with no lag, for three types of control a_n , $a_n - \dot{\theta}$, and $a_n + \ddot{\theta}$ are shown in figure 3. The results for all three types of control are similar in that, as the airspeed is decreased for a constant gain setting, there is a large decrease in response below the steady-state command value because of the effect of the maneuvering stability of the airplane. It can also be seen from figure 3 that to approach zero steady-state error would require high forward-loop gains which obviously can lead to stability problems if power-control lags are considered. In any of the systems considered, it would be necessary to vary the gain with flight condition, that is, with airspeed, altitude, and center-of-gravity location.

In order to obtain an idea of the effect of power-control dynamics on the performance of the control systems, inverse Nyquist plots were made by utilizing the transfer functions of the various components. The power control was assumed to be a second-order system with a natural frequency of about 30 radians per second and a damping ratio of about 0.5. A comparison of the Nyquist plots, where power-control characteristics were assumed to be perfect, with the characteristics of a more practical power control, showed that the addition of power-control dynamics lowered the forward-loop gain that was consistent with stability requirements considerably below the value that would be required to obtain satisfactory performance. By plotting the closed-loop frequency responses for any given flight condition from the inverse Nyquist plots, an idea of the transient response of the system can be obtained. Frequency responses thus obtained showed a decided dip at frequencies less than the resonant frequency peak. This type of frequency response generally indicates the presence of two modes of motion. One mode would have the characteristics associated with a system having low natural frequency and high damping, and the other mode would be the characteristic system having a higher natural frequency and low damping. The long response time and large overshoot would make this type of system unacceptable for use as an acceleration restrictor.

Since the addition of power-control dynamics apparently caused the deterioration in performance, the addition of a compensating network to

offset the lagging phase angle introduced by the power control suggests itself. As mentioned previously and shown in figure 3, it appears desirable to include in the network an integrating characteristic in order to maintain zero steady-state error. The Nyquist analysis indicated the general characteristics of the compensating network required. The transfer function of the network used is as follows:

$$\frac{\text{Output}}{\text{Input}} = \frac{0.19(1 + 0.14j\omega)(1 + 0.08j\omega)}{j\omega(1 + 0.0036j\omega)^2}$$

Logarithmic plots of amplitude and phase angle obtained with this network are shown in figure 4.

Typical results with the $a_n + \ddot{\theta}$ control for the various flight conditions at sea level are shown in figure 5. The values of the gains K_1 and K_2 were adjusted to give about optimum response for each condition. In all cases the command rate of normal acceleration was 6g per second. The results shown in figure 5 indicate that this system is an excellent acceleration restrictor as the overshoot in most cases is less than 0.1g. It was found, however, that the gain changes in the pitching-acceleration loop were very critical. Figure 6 illustrates the transient responses for a given flight condition and constant forward-loop gain K_1 . It can be seen that with no $\ddot{\theta}$ feedback this particular control performs satisfactorily and there is very little change as the gain K_2 is changed from 0 to 0.01; however, there is a marked change when the gain is increased to 0.015. A further small increase makes the system unstable. Results for the airplane with reduced damping at an altitude of 20,000 feet were unacceptable in all cases because of stability problems and the large overshoots encountered. It appears from figures 5 and 6 that the use of positive pitching-acceleration feedback alone would not be acceptable with the airplane-control-system combination studied. The reasons for this conclusion are the instability of this type of control at an altitude of 20,000 feet and the critical nature of the inner-loop feedback gain.

Figure 7 shows the best performance obtained, with any possible combination of the various feedbacks, for the flight conditions considered. Figure 7(a) is for a speed of 600 feet per second at sea level and three center-of-gravity locations. These results show that the performance is satisfactory when the various gains are changed with flight condition. Similar results are shown in figures 7(b), (c), and (d) for different airspeeds, damping, and altitudes. In all cases the elevator deflection required and the rate of elevator motion required, if 6g per second is assumed to be the maximum input rate of normal acceleration, were within practical limits for current airframes and power-control systems.

In general, best results were obtained by using the $a_n - \ddot{\theta} - \dot{\theta}$ control. The use of $a_n - \dot{\theta}$ control generally reduced the allowable value of the forward-loop gain so that the response time was increased to an unacceptable degree.

One particular set of gains used in the $a_n - \ddot{\theta} - \dot{\theta}$ control ($K_1 = 0.3$, $K_2 = -0.01$, and $K_3 = -0.2$) was found satisfactory over a wide range of conditions. Figure 8 shows how the output acceleration varies with flight condition when the inner- and outer-loop gains are held constant.

Gust Alleviation Results

In order to obtain some knowledge of the effects of turbulent air on the airplane-control-system combinations under investigation, frequency responses due to sinusoidal gusts were calculated. Unsteady lift was neglected in the calculations inasmuch as it is believed that its effects would be to attenuate the response at the higher frequencies. The calculated gust responses for the $a_n - \dot{\theta}$ and $a_n + \ddot{\theta}$ systems and for the basic airplane are presented in figure 9. At the lower frequencies, where the gust power in the atmosphere is the greatest, the $a_n + \ddot{\theta}$ control shows the greatest reduction in acceleration response to gusts as the forward-loop gain K_1 is increased. A considerable reduction in acceleration response is also shown by the $a_n - \dot{\theta}$ control. With either type of control, a large increase in pitching accompanies the reduction in normal acceleration. This pitching results from the attempt of the normal-acceleration control to maintain the lift, and hence the angle of attack, at a constant value during flight through gusts. The expected effect of the pitching-velocity feedback in reducing the pitching motion is not very apparent for the larger values of K_1 . With the practical systems shown in figure 10, the simulated rough-air input was obtained by integrating the output from the motor-driven cam as previously mentioned in the section entitled "Analysis." A repeatable cyclic input was desired so that at any given flight condition a direct comparison could be made between the response of the basic airplane and the response of the airplane with the different normal-acceleration control systems. The effects of changes in the inner-loop feedback quantities and gain changes in both outer and inner loops can be seen easily with a repeatable input. Figure 10 presents the normal-acceleration and pitching-velocity responses to the rough-air input for the basic airplane with one forward and one rearward center-of-gravity location at an airspeed of 1,000 feet per second. For comparison, typical results are presented for the $a_n + \ddot{\theta}$ controlled airplane with a

forward and a rearward center-of-gravity location and for the $a_n - \ddot{\theta} - \dot{\theta}$ controlled airplane with a rearward center-of-gravity location. The inner- and outer-loop gains associated with the $a_n + \ddot{\theta}$ control and the $a_n - \ddot{\theta} - \dot{\theta}$ control in figure 10 correspond to optimum gains shown in figures 5 and 7, respectively. No attempt was made to vary systematically the feedback combinations and gain values to try to improve the responses to rough air.

The various control systems generally appeared to reduce the response of the airplane to gusts less than might have been expected from the ideal $a_n + \ddot{\theta}$ control of figure 9. Stability requirements dictated a considerably lower forward-loop gain K_1 for the practical $a_n + \ddot{\theta}$ system than is indicated for the ideal $a_n + \ddot{\theta}$ control of figure 9. The addition of a compensating network with an integrating characteristic in the practical control system precludes a direct comparison between the gains of the ideal and practical systems. It is possible, however, to compare the gains at other than zero frequency. For example, consider the practical $a_n + \ddot{\theta}$ system of figure 5 for a maneuver margin of 3.3 percent of the mean aerodynamic chord, an airspeed of 600 feet per second at sea level, and a forward-loop gain K_1 of 0.05. For these conditions the natural frequency of the basic airplane is about 6 radians per second. The amplitude ratio or gain of the compensating network at this frequency is about 0.06 (-24 decibels, from fig. 4). Combining the K_1 value of 0.05 with the compensating network gain of 0.06 results in an effective K_1 value of about 0.003. A check of the ideal $a_n + \ddot{\theta}$ system for the same conditions (see fig. 9), that is, $K_1 = 0.003$, indicates that even the ideal system at this gain offers very little reduction in normal-acceleration response to gusts. In the ideal $a_n + \ddot{\theta}$ control system a value of K_1 of about 0.15 would yield an appreciable reduction in normal-acceleration response to gusts as compared with the basic airplane at low frequencies where the gust power is the greatest. For the same conditions a practical system would require a value of K_1 of about 2.5, which is much higher than the value of 0.05 actually obtained.

With the various systems, however, there is a definite reduction in the normal-acceleration response at the lower frequencies as compared with that of the basic airplane when the maneuver margin is small. Also, the magnitude of pitching-velocity response is definitely greater for the controlled airplane than for the basic airplane. These observations are not based on any systematic analysis of the time histories, such as a spectral-density analysis, but on visual study of time histories, several of which are shown in figure 10.

CONCLUDING REMARKS

A theoretical analysis was made to determine the performance and acceleration-restriction capabilities of a normal-acceleration control system in a typical subsonic jet fighter airplane. Several combinations of the inner-loop feedback quantities, pitching velocity and pitching acceleration, were investigated in combination with normal-acceleration feedback. The flight conditions considered were airspeeds of 600 and 1,000 feet per second at sea level and at 20,000 feet and maneuver margins of 3.3, 13.3, and 23.3 percent of the mean aerodynamic chord. At 20,000 feet the damping derivatives of the basic airplane were reduced to one-half the values used at sea level.

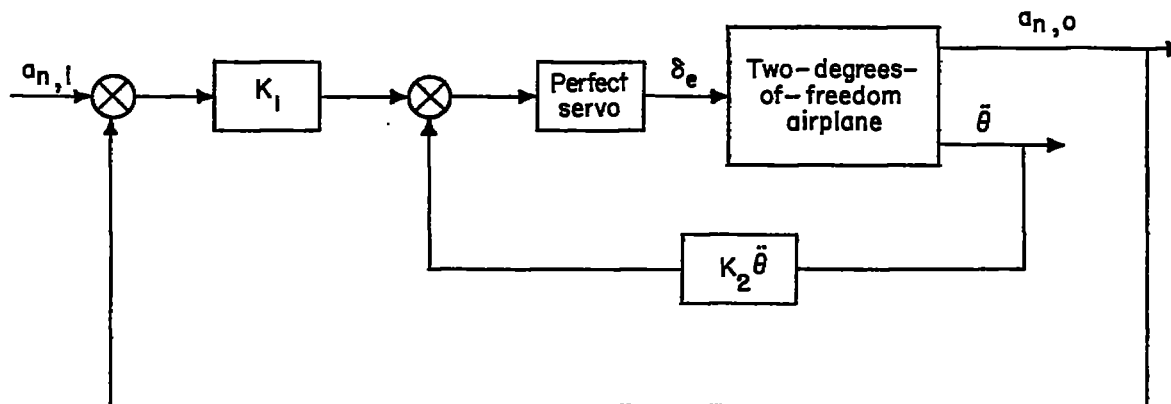
A normal-acceleration control system with negative feedback of pitching velocity and pitching acceleration was found to restrict the normal acceleration to within 10 percent of the desired value for the flight conditions considered. In order to achieve this result a compensating network, which reduced the phase lag in the vicinity of the natural frequency of the power control, was required. It was also necessary to vary the gains with varying flight conditions.

The effects of simulated rough air on the airplane—control-system combinations were also investigated. The normal-acceleration response of the controlled airplane to rough air was somewhat reduced as compared with that of the basic airplane, particularly at the lower maneuver margins. The magnitude of the pitching-velocity response was greater for the controlled airplane, as might be expected.

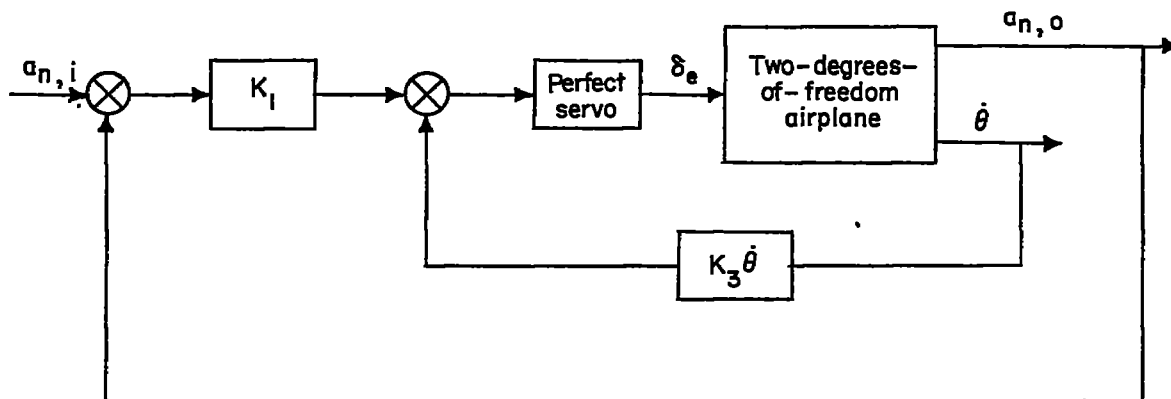
Langley Aeronautical Laboratory,
National Advisory Committee for Aeronautics,
Langley Field, Va., September 19, 1957.

REFERENCES

1. Phillips, William H.: Theoretical Analysis of Some Simple Types of Acceleration Restrictors. NACA TN 2574, 1951.
2. Assadourian, Arthur: Operating Characteristics of an Acceleration Restrictor As Determined by Means of a Simulator. NACA TN 3319, 1954.
3. Kraft, Christopher C., Jr.: Theoretical Analysis of an Airplane Acceleration Restrictor Controlled by Normal Acceleration, Pitching Acceleration, and Pitching Velocity. NACA TN 3243, 1954.
4. Stokes, Fred H., and Mathews, Charles W.: Theoretical Investigation of Longitudinal Response Characteristics of a Swept-Wing Fighter Airplane Having a Normal-Acceleration Control System and a Comparison With Other Types of Systems. NACA TN 3191, 1954.
5. Chilton, Robert G.: Some Measurements of Atmospheric Turbulence Obtained From Flow-Direction Vanes Mounted on an Airplane. NACA TN 3313, 1954.



(a) $a_n + \ddot{\theta}$ control.



(b) $a_n - \dot{\theta}$ control.

Figure 1.- Block diagrams for ideal control systems.

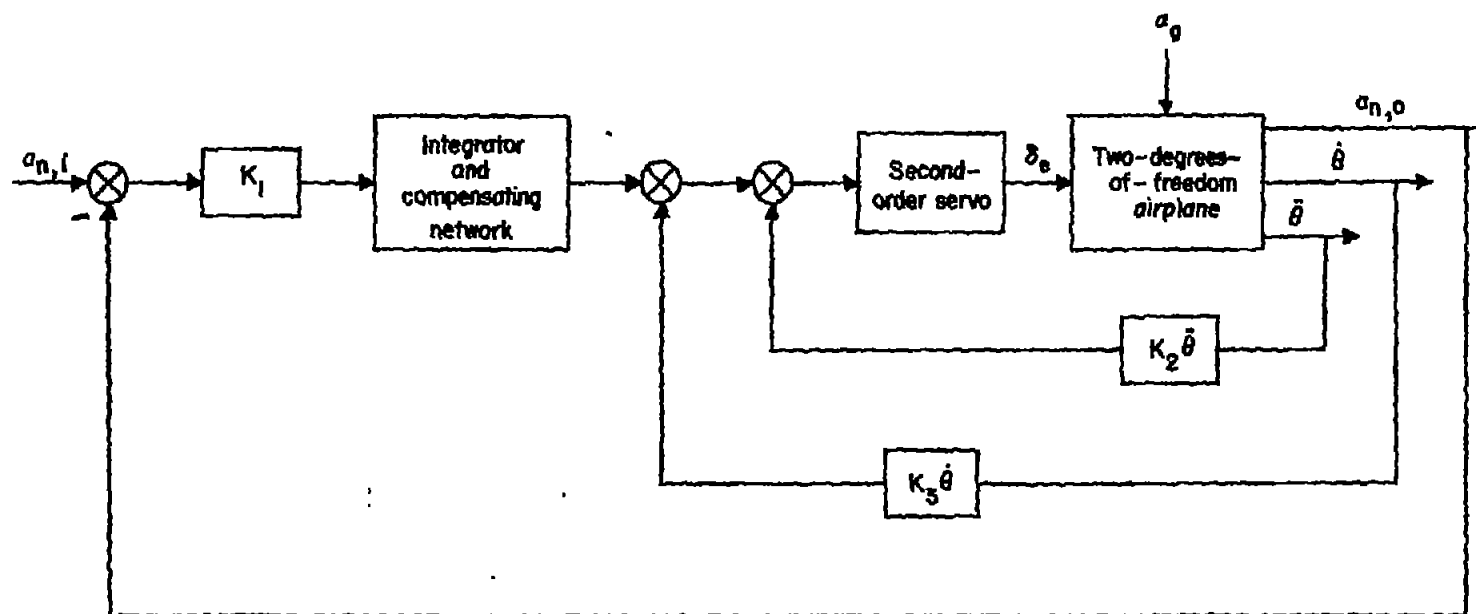
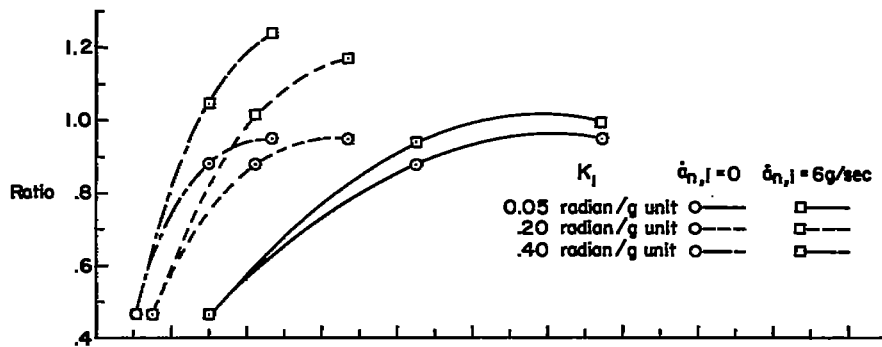
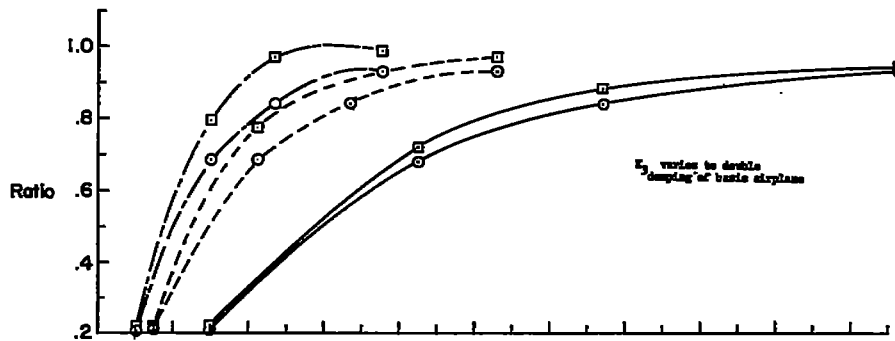


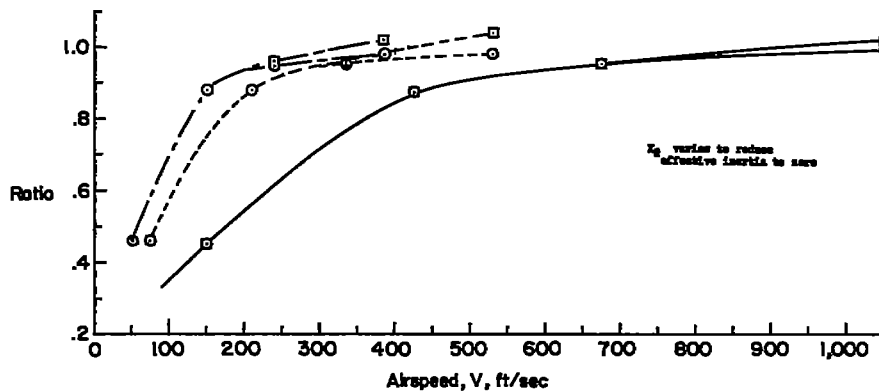
Figure 2.- Composite block diagram of complete system. This system was investigated with no inner-loop feedback as well as with all combinations, both positive and negative, of the inner-loop feedbacks.



(a) a_n control.



(b) $a_n - \dot{\theta}$ control.



(c) $a_n + \ddot{\theta}$ control.

Figure 3.- Ratio of peak and steady-state normal acceleration to command acceleration for ideal control systems. Maneuver margin, 3.3 percent of the mean aerodynamic chord.

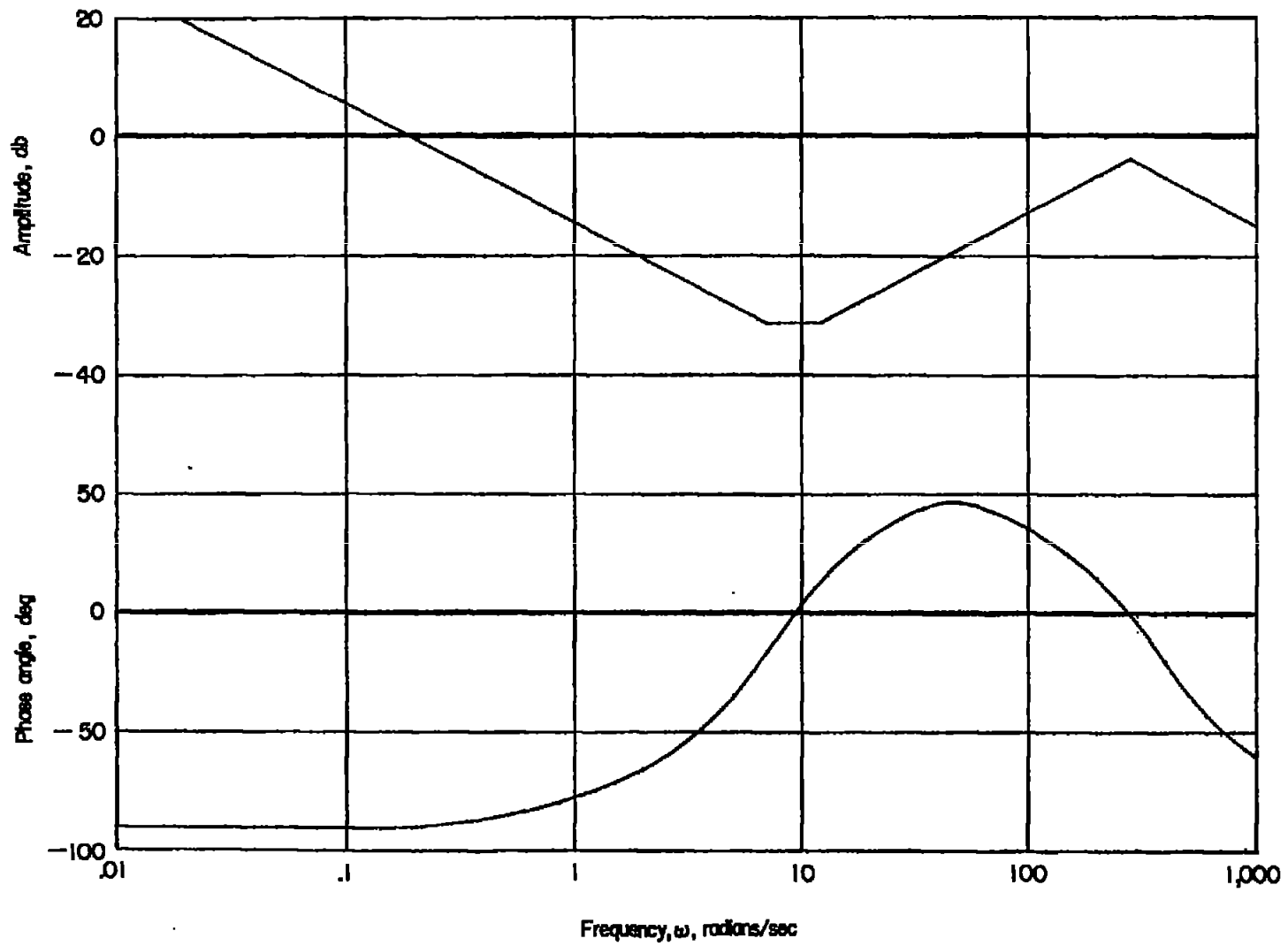
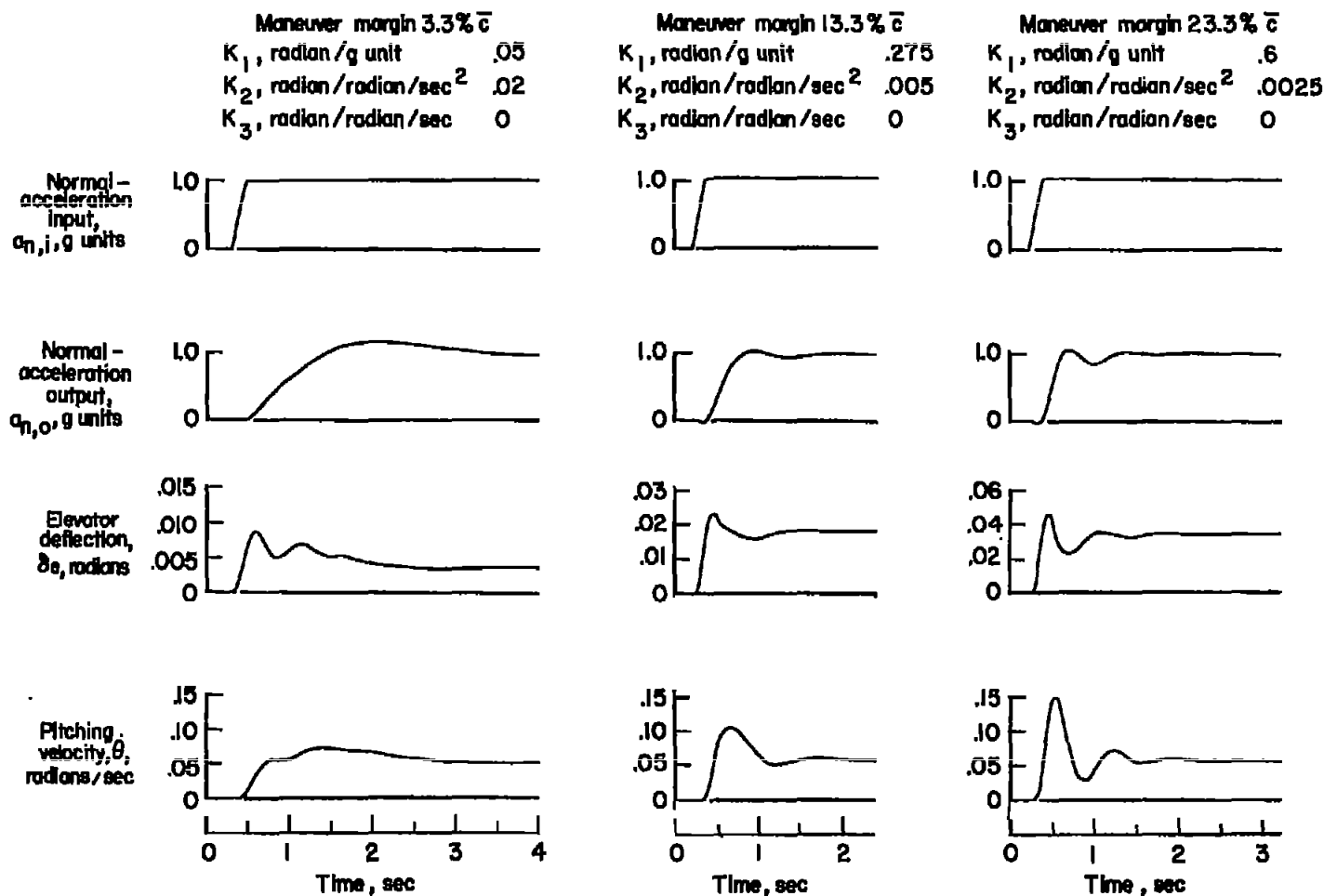
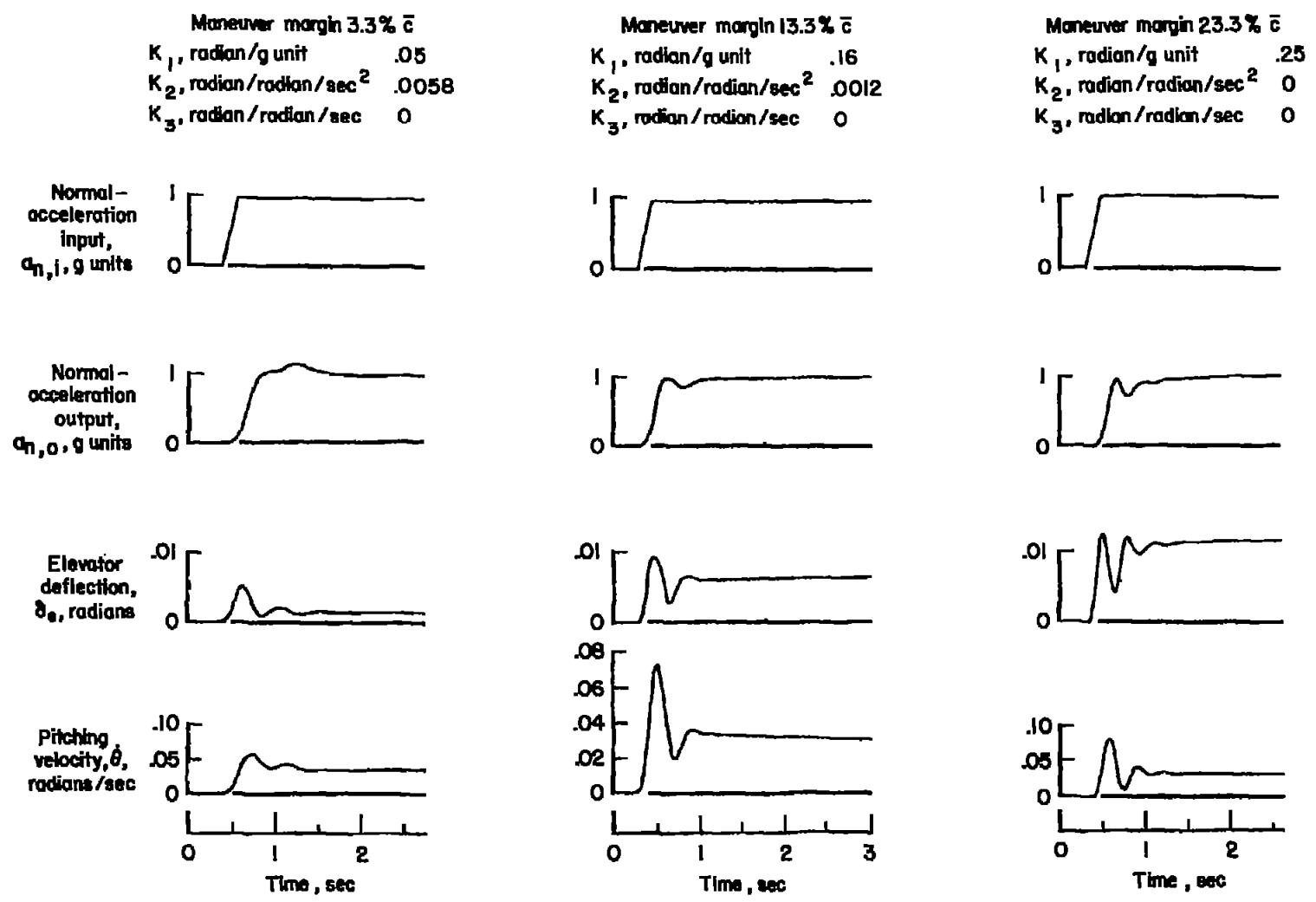


Figure 4.- Approximate attenuation and phase-angle curves for compensating network.



(a) $V = 600$ feet per second; sea level.

Figure 5.- Time histories of command input and corresponding transient responses for $a_n + \dot{\theta}$ control.



(b) $V = 1,000$ feet per second; sea level.

Figure 5.- Concluded.

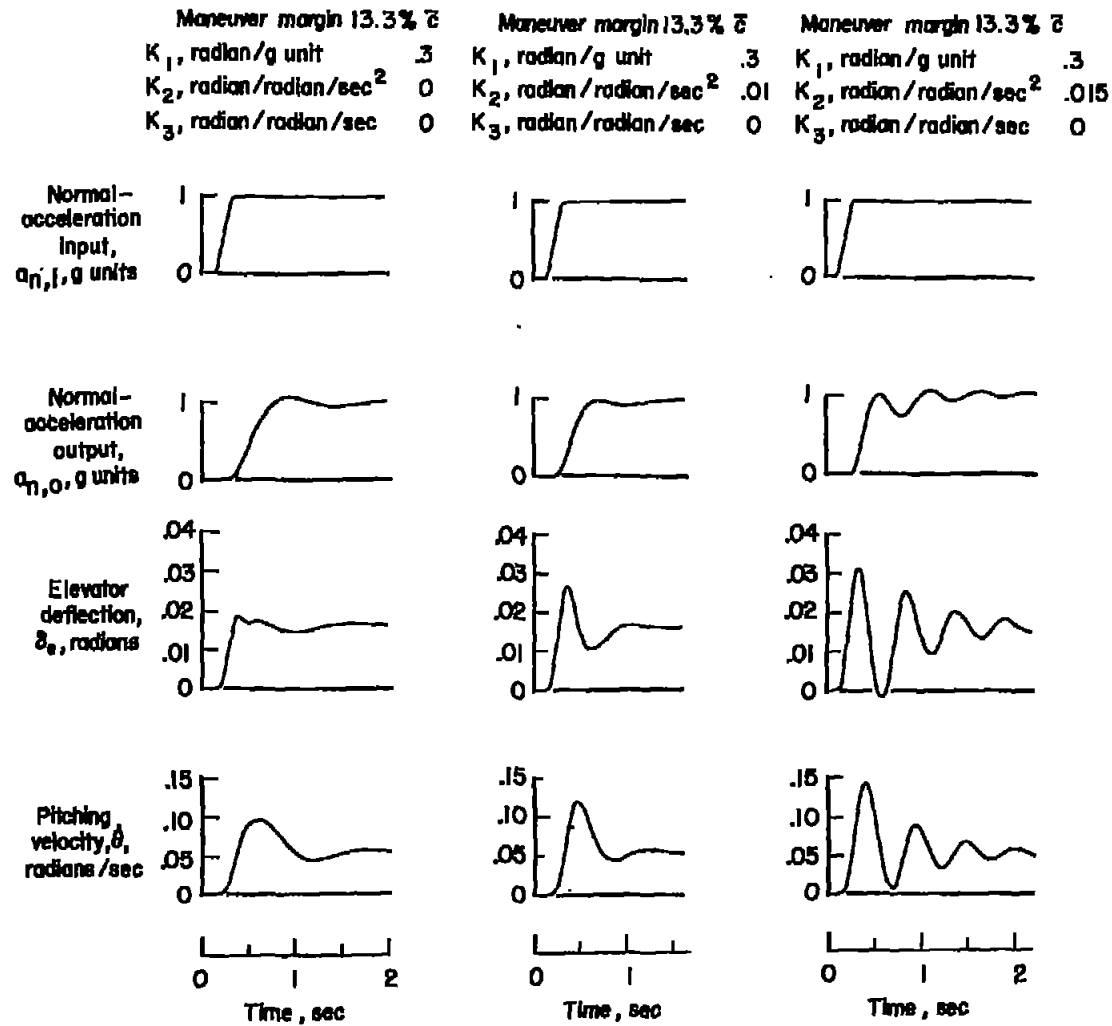
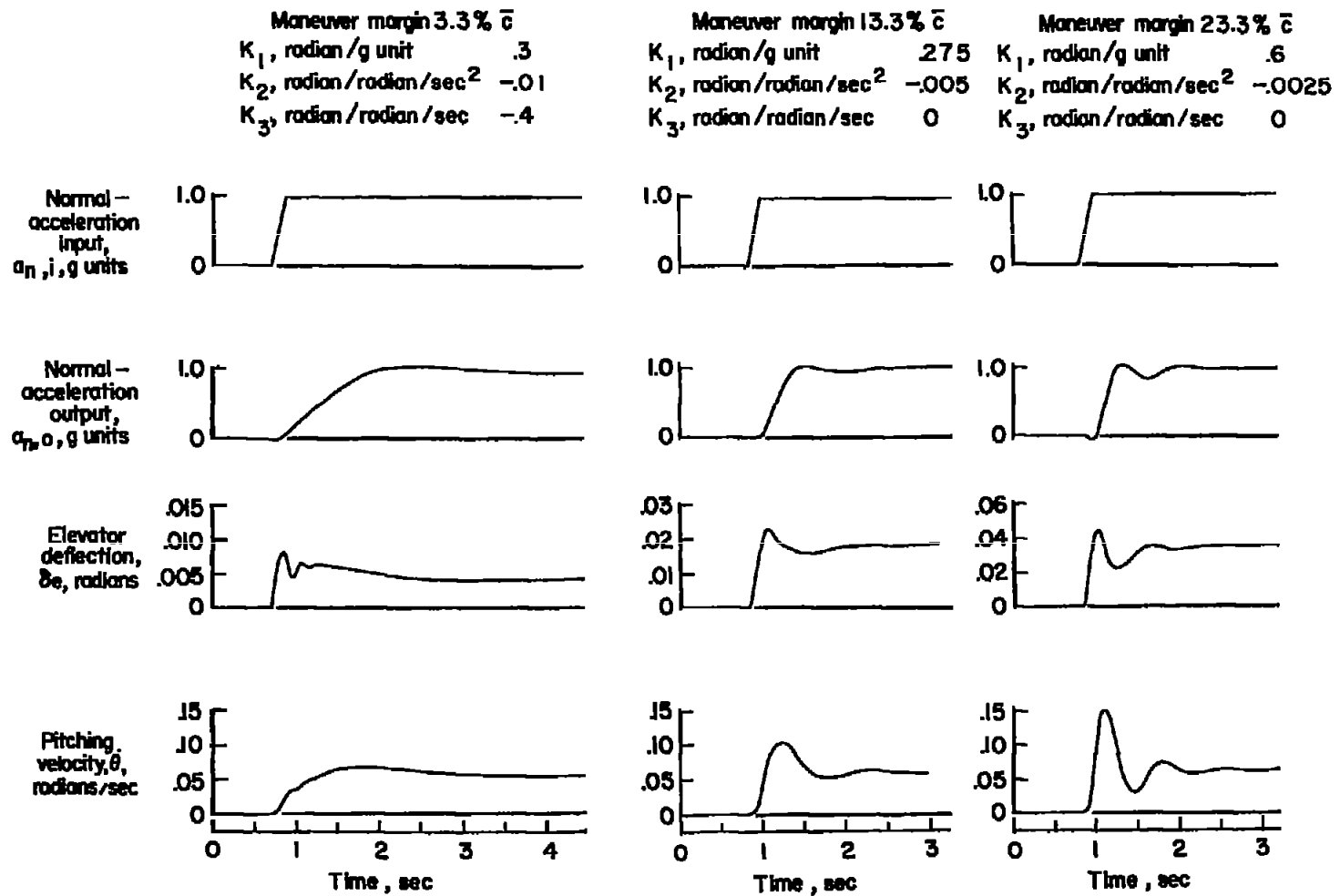
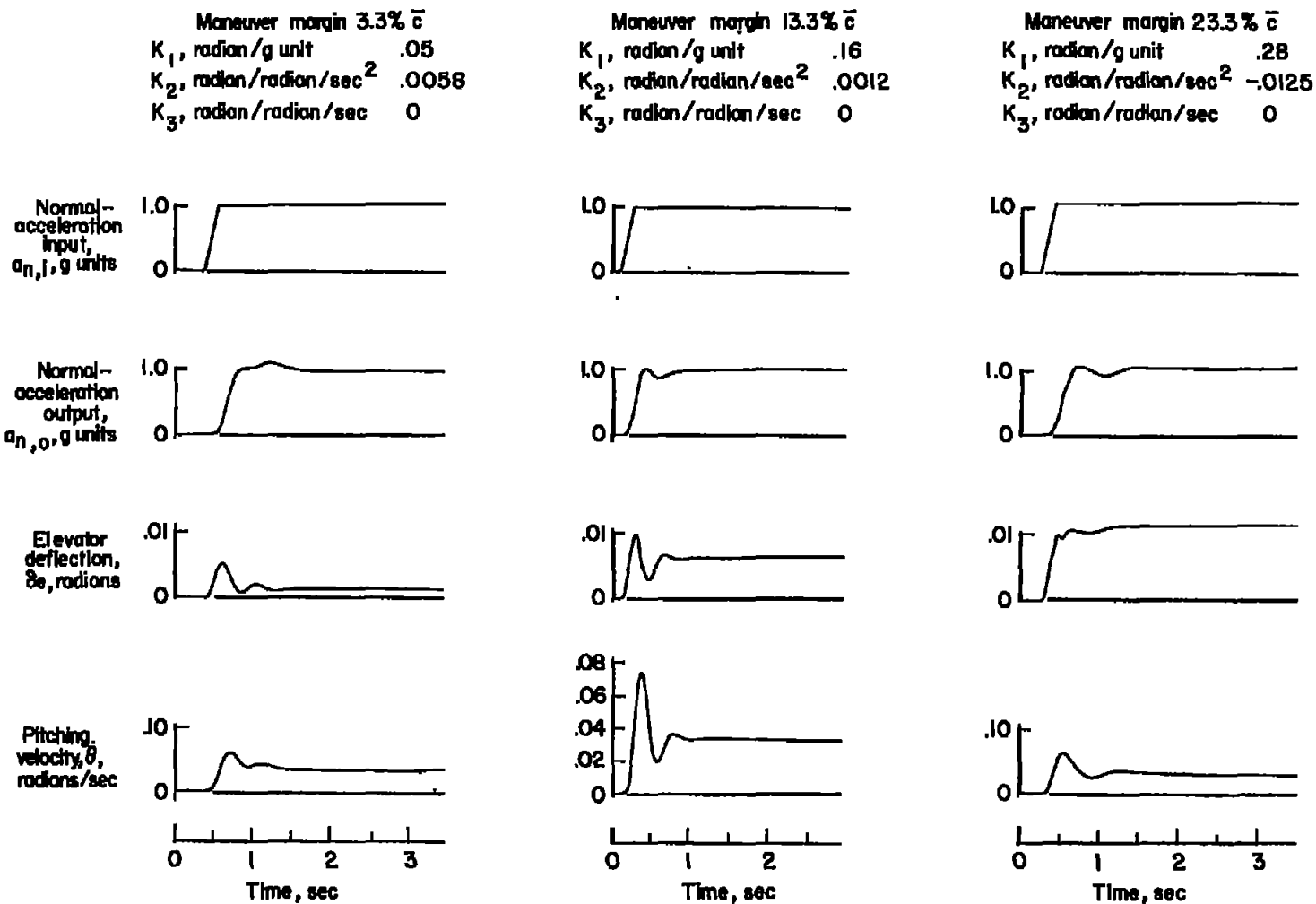


Figure 6.- Time histories of command input and corresponding transient responses for the $a_n + \dot{\theta}$ control, showing the effect of changing the inner-loop gain K_2 .



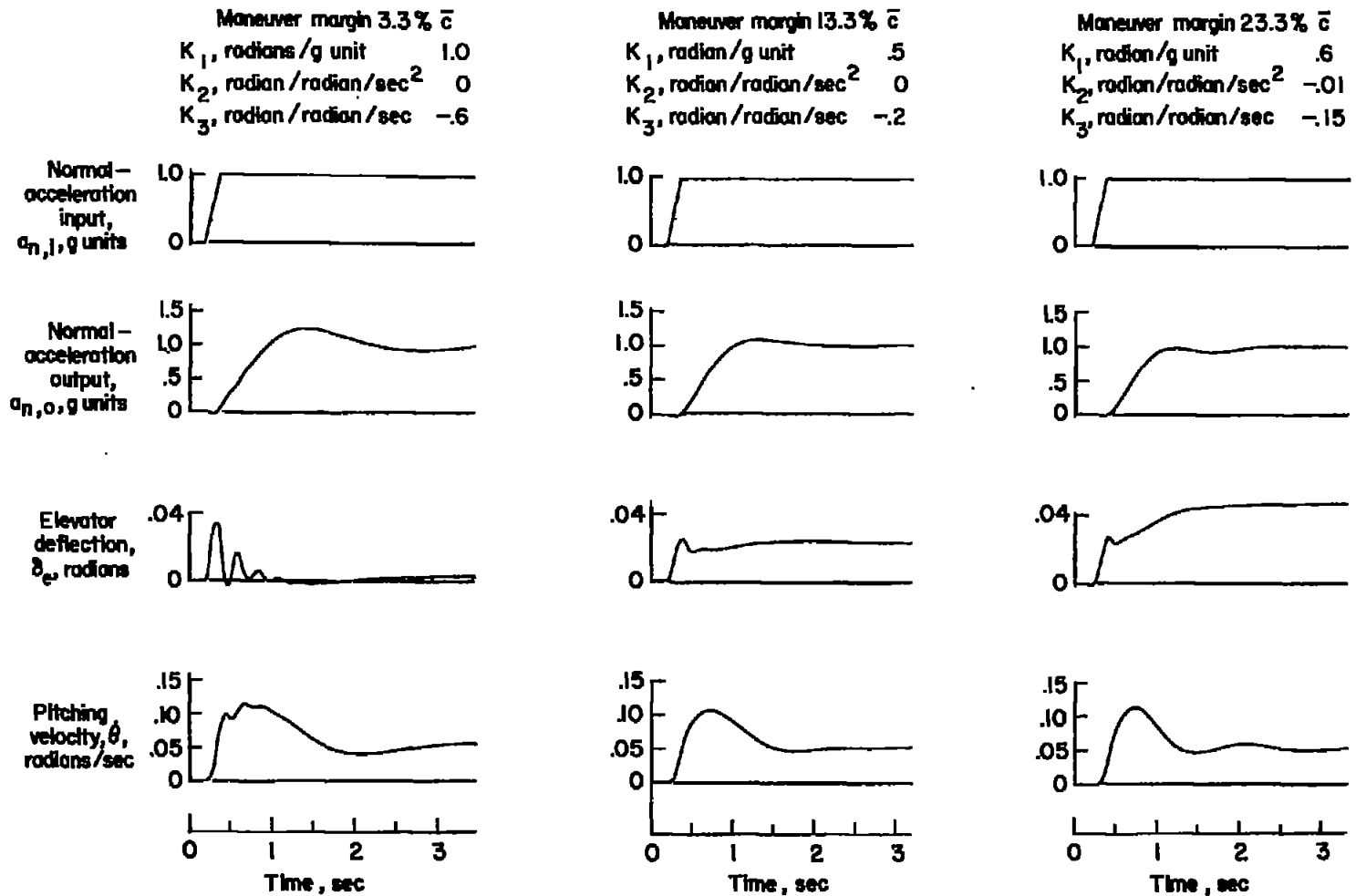
(a) $V = 600$ feet per second; sea level. Note that δ_e scales are different.

Figure 7.- Time histories of command input and corresponding optimum transient responses that were obtained.



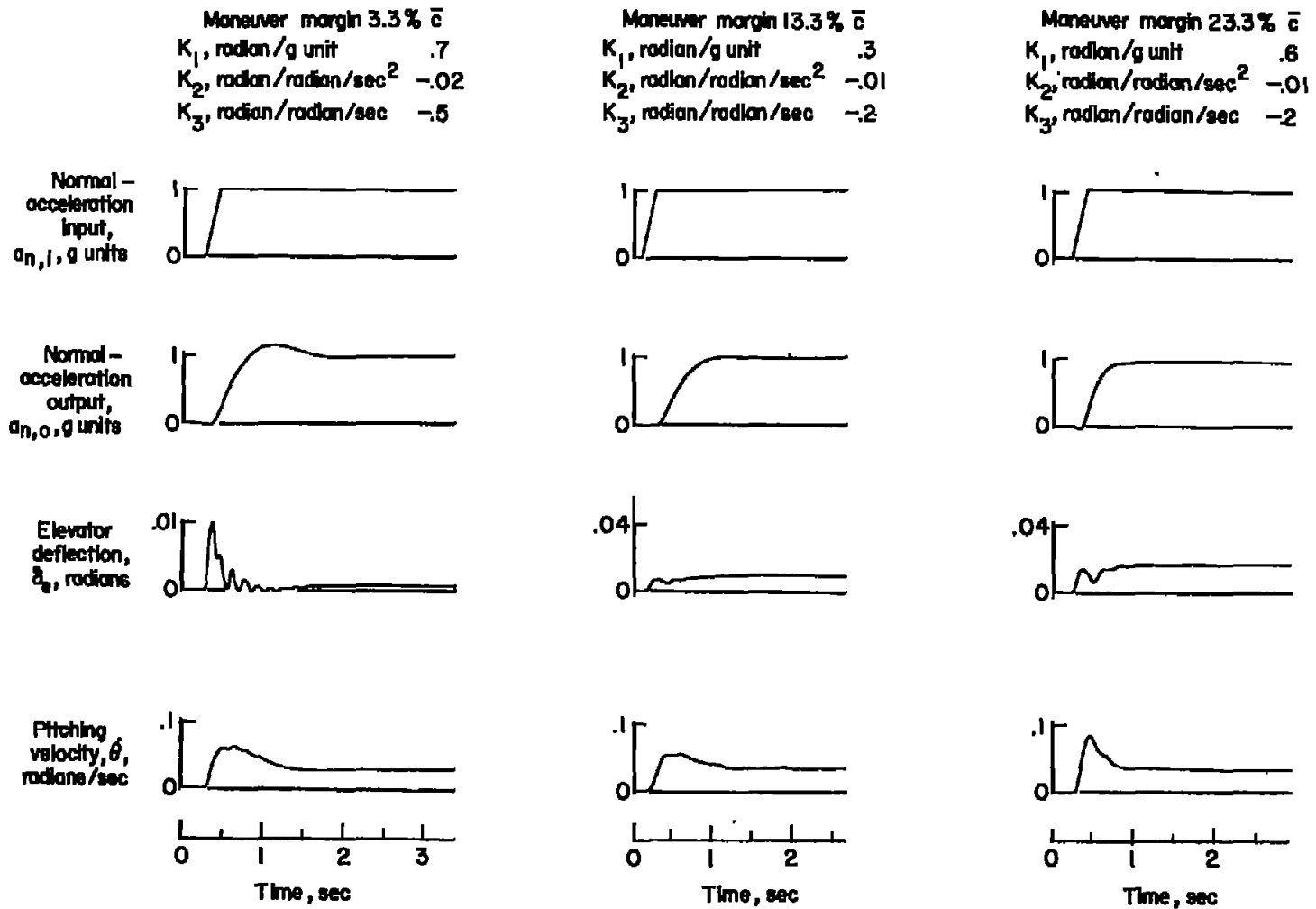
(b) $V = 1,000$ feet per second; sea level. Note that $\dot{\theta}$ scales are different.

Figure 7.- Continued.



(c) $V = 600$ feet per second; altitude, 20,000 feet.

Figure 7.- Continued.



(d) $V = 1,000$ feet per second; altitude, 20,000 feet. Note that δ_e scales are different.

Figure 7.- Concluded.

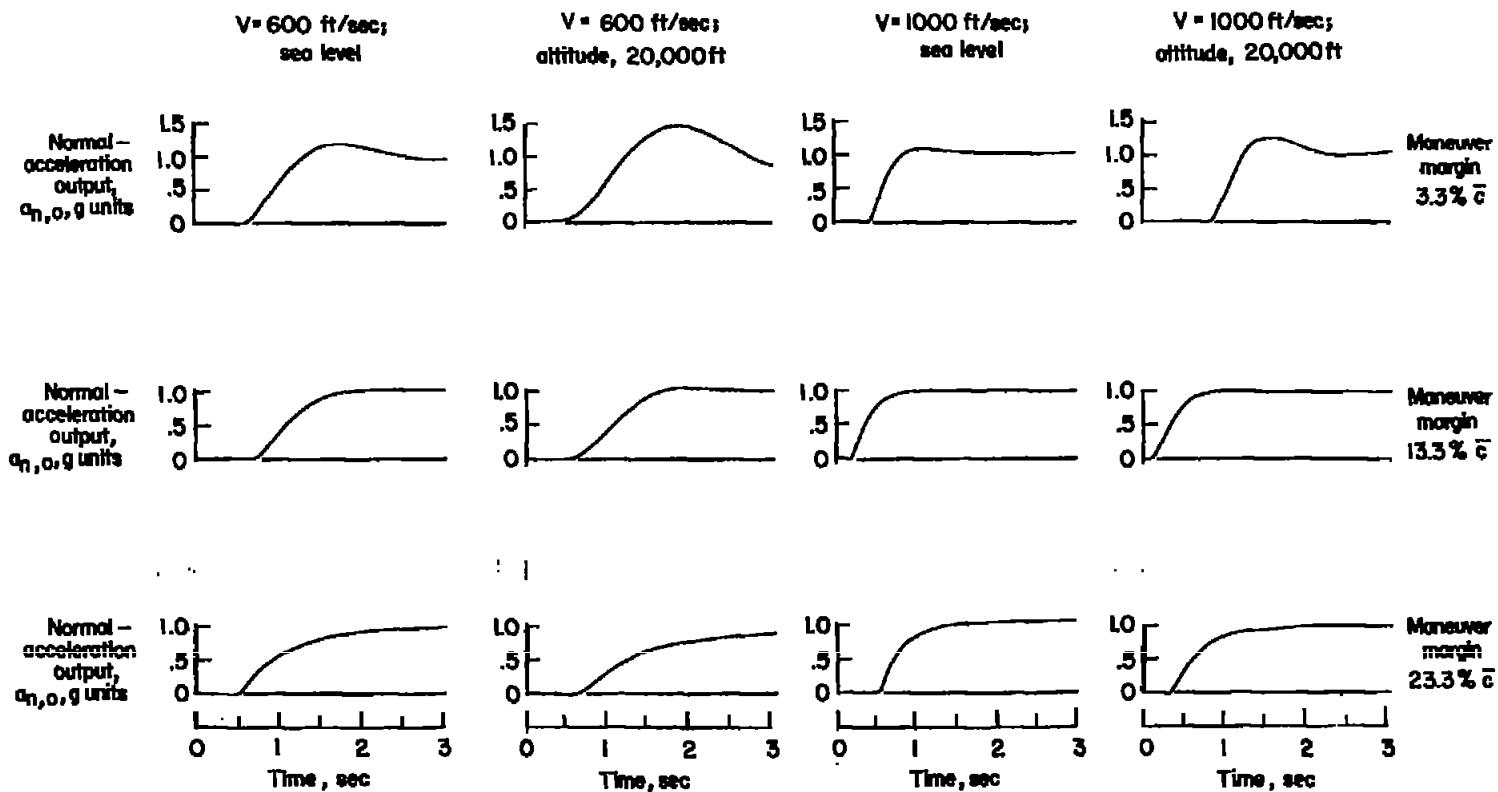
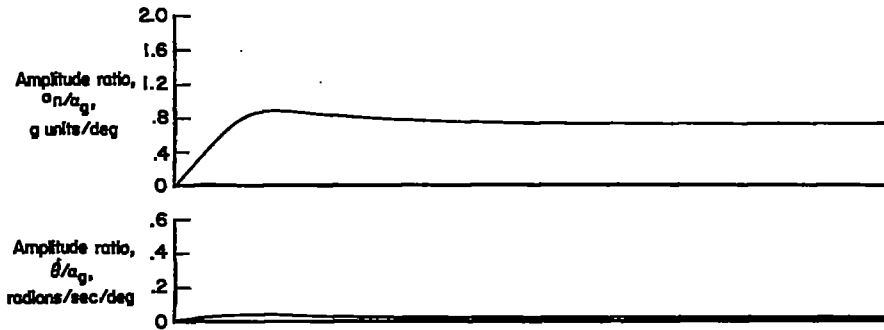
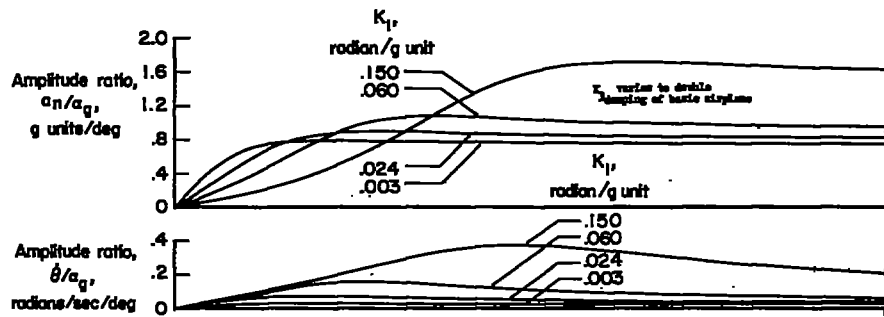


Figure 8.- Time histories showing transient normal-acceleration responses where type of control and magnitude of gains remained constant throughout the flight conditions investigated.

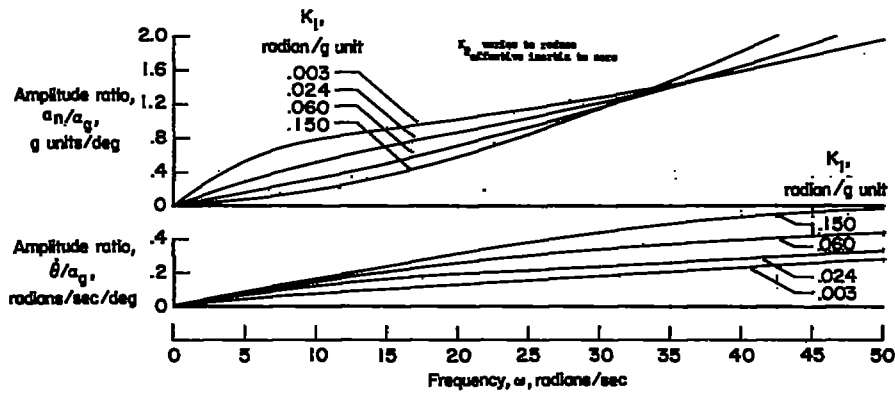
$$K_1 = 0.3; K_2 = -0.01; K_3 = -0.2.$$



(a) Basic airplane.



(b) $a_n - \dot{\theta}$ control.



(c) $a_n + \ddot{\theta}$ control.

Figure 9.- Frequency responses for basic airplane and controlled airplane due to change in angle of attack caused by rough air. $V = 600$ feet per second; sea level; maneuver margin, 3.3 percent of mean aerodynamic chord.

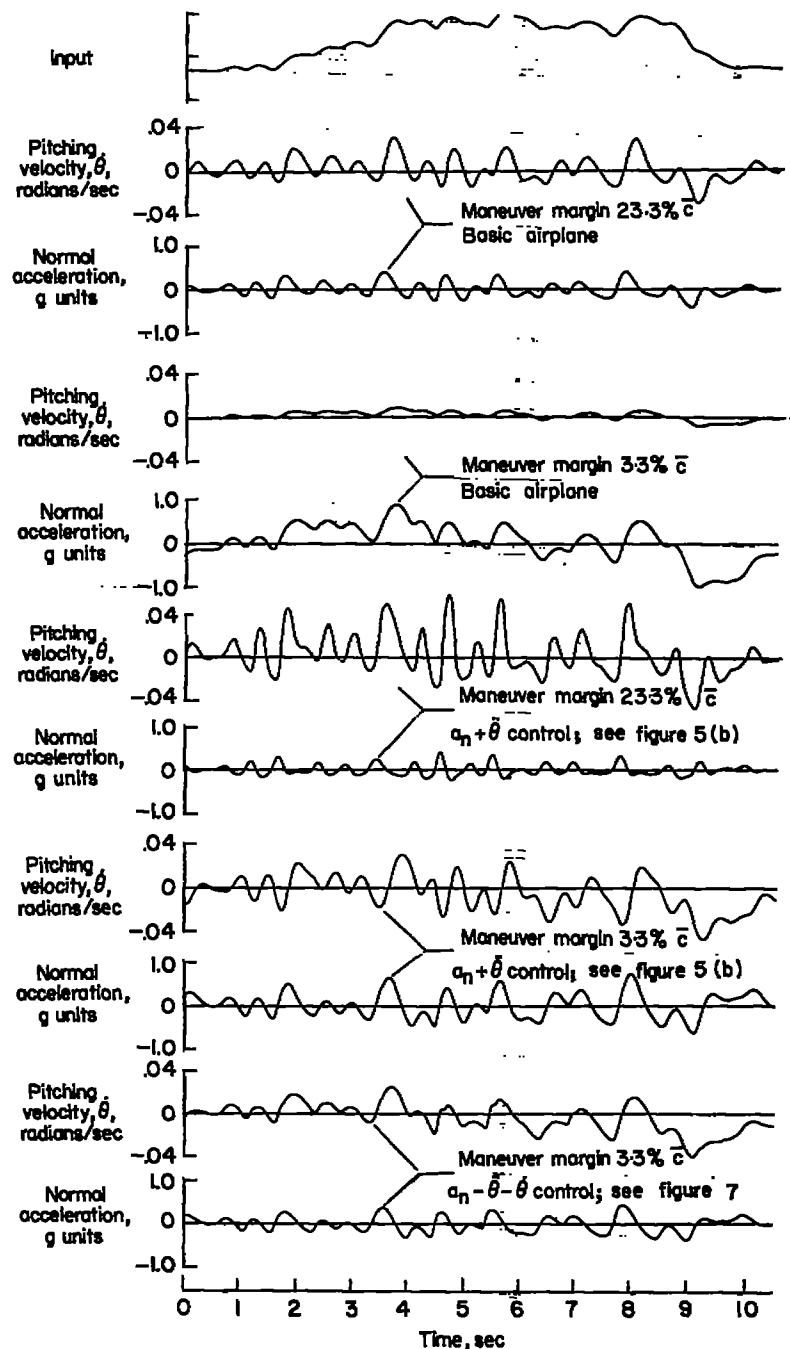


Figure 10.- Time histories of simulated rough-air input and corresponding typical basic-airplane and controlled-airplane responses. $V = 1,000$ feet per second; sea level.